HHS Public Access

Author manuscript

ACS Biomater Sci Eng. Author manuscript; available in PMC 2023 January 14.

Published in final edited form as:

ACS Biomater Sci Eng. 2022 June 13; 8(6): 2518–2525. doi:10.1021/acsbiomaterials.2c00284.

Injectable Hydrogel Containing Cowpea Mosaic Virus Nanoparticles Prevents Colon Cancer Growth

Christian Isalomboto Nkanga,

Department of NanoEngineering, University of California San Diego, La Jolla, California 92039, United States; Present Address: Department of Medicinal Chemistry and Pharmacognosy, Faculty of Pharmaceutical Sciences, University of Kinshasa, B.P. 212, Kinshasa, XI, Democratic Republic of the Congo (C.I.N.)

Nicole F. Steinmetz

Department of NanoEngineering, Department of Bioengineering, Department of Radiology, Center for Nano-ImmunoEngineering, Moores Cancer Center, and Institute for Materials Discovery and Design, University of California San Diego, La Jolla, California 92039, United States

Abstract

Despite advances in laparoscopic surgery combined with neoadjuvant and adjuvant therapy, colon cancer management remains challenging in oncology. Recurrence of cancerous tissue locally or in distant organs (metastasis) is the major problem in colon cancer management. Vaccines and immunotherapies hold promise in preventing cancer recurrence through stimulation of the immune system. We and others have shown that nanoparticles from plant viruses, such as cowpea mosaic virus (CPMV) nanoparticles, are potent immune adjuvants for cancer vaccines and serve as immunostimulatory agents in the treatment or prevention of tumors. While being noninfectious toward mammals, CPMV activates the innate immune system through recognition by pattern recognition receptors (PRRs). While the particulate structure of CPMV is essential for prominent immune activation, the proteinaceous architecture makes CPMV subject to degradation *in vivo*; thus, CPMV immunotherapy requires repeated injections for optimal outcome. Frequent intraperitoneal (IP) injections however are not optimal from a clinical point of view and can worsen the patient's quality of life due to the hospitalization required for IP administration. To overcome the need for repeated IP injections, we loaded CPMV nanoparticles in injectable chitosan/glycerophosphate (GP) hydrogel formulations, characterized their slow-release potential, and assessed the antitumor preventative efficacy of CPMV-in-hydrogel single dose *versus* soluble

Corresponding Author: **Nicole F. Steinmetz** – *Department of NanoEngineering, Department of Bioengineering, Department of Radiology, Center for Nano-ImmunoEngineering, Moores Cancer Center, and Institute for Materials Discovery and Design, University of California San Diego, La Jolla, California 92039, United States;* nsteinmetz@ucsd.edu.

The authors declare the following competing financial interest(s): Dr. N. F. Steinmetz is a co-founder of, has equity in, and has a financial interest with Mosaic ImmunoEngineering Inc.; Dr. N. F. Steinmetz serves as the Director, Board Member, Acting Chief Scientific Officer, and paid consultant to Mosaic. Dr. C. I. Nkanga declares no potential conflicts of interest.

Supporting Information

The Supporting Information is available free of charge at https://pubs.acs.org/doi/10.1021/acsbiomaterials.2c00284.
Detailed methods; characterization of Cy5-conjugated CPMV; characterization of CPMV released from hydrogels (DLS, SEC, TEM); and biodistribution and body weight (PDF)

Complete contact information is available at: https://pubs.acs.org/10.1021/acsbiomaterials.2c00284

CPMV (single and prime-boost administration). Using fluorescently labeled CPMV-in-hydrogel formulations, *in vivo* release data indicated that single IP injection of the hydrogel formulation yielded a gel depot that supplied intact CPMV over the study period of 3 weeks, while soluble CPMV lasted only for one week. IP administration of the CPMV-in-hydrogel formulation boosted with soluble CPMV for combined immediate and sustained immune activation significantly inhibited colon cancer growth after CT26 IP challenge in BALB/c mice. The observed antitumor efficacy suggests that CPMV can be formulated in a chitosan/GP hydrogel to achieve prolonged immunostimulatory effects as single-dose immunotherapy against colon cancer recurrence. The present findings illustrate the potential of injectable hydrogel technology to accommodate plant virus nanoparticles to boost the translational development of effective antitumor immunotherapies.

Graphical Abstract

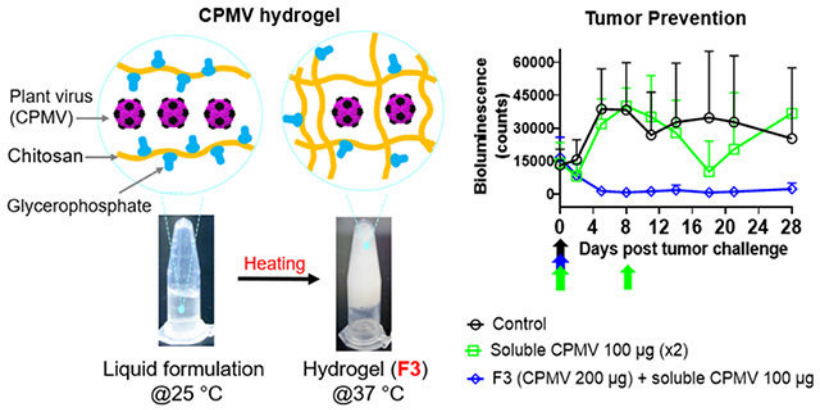

Keywords

plant virus; cowpea mosaic virus; chitosan; thermosensitive hydrogels; in situ forming depot; colon cancer recurrence; antitumor immunotherapy

1. INTRODUCTION

Colon cancer represents the second leading cause of cancer-related deaths and the third most common cancer in terms of new cases.[1] In 2020, there were 935 000 deaths and 1.93 million cases of colon cancer globally.[2] These statistics are enormous considering the limited accessibility to healthcare setting patients may have faced over the last two years due to the coronavirus disease 2019 (COVID-19) pandemic;[3] the serial lockdowns coordinated worldwide during the pandemic in 2020 might have reduced access to diagnosis and treatment facilities, likely leading to underestimation of cancer incidence statistics. Poor cancer screening combined with ineffective control of risk factors and treatment limitations are among the factors that worsen cancer mortality and morbidity globally, especially in developing countries.[4] The mainstay of the treatment for colon cancer is laparoscopic surgery combined with preoperative or postoperative adjuvant chemotherapy and radiotherapy.[5] However recurrence occurs at a rate of 70% within 2 years and 90%

within 5 years after surgery.[6] Therefore, there is need to develop treatments to prevent recurrence.

Over the last two decades, immunotherapies have shown some success against metastatic colon cancer, with clinical approval of monoclonal antibodies such as cetuximab and panitumumab, which are antiepidermal growth factor receptor (EGFR) antibodies.[7] In the preclinical setting, we have shown that *in situ* vaccination immunotherapy using immunostimulatory cowpea mosaic virus (CPMV) nanoparticles is a promising strategy for cancer therapy: CPMV is a 30 nm-sized icosahedral, nonglycosylated plant virus with a bipartite RNA genome that—while being noninfectious toward mammals—triggers potent innate immune activation through recognition by pattern recognition receptors (PRRs).[8] We have demonstrated that CPMV elicits potent systemic and durable antitumor immunity through priming the innate immune system; efficacy has been reported in mouse models of colon cancer[9,10] and other tumor models[11,12] and in canine patients.[13] In recent work, we also demonstrated that CPMV targeted to the lungs primes innate immune activation and therefore protects from the onset of lung metastasis.[14] Mechanistically, CPMV modulates the tumor microenvironment (TME) by activating the innate immune cells (switch of M2 to M1 macrophages), recruitment and activation of natural killer (NK) cells, dendritic cells (DCs), and N1 neutrophils, thereby initiating a cascade of tumor cell killing mechanisms, resulting in efficient presentation of both tumor-associated and neoantigens, and generation of a functionally active adaptive antitumor immunity via tumor antigen-specific $CD4^{\pm}$ and $CD8^{\pm}$ effector and memory T cells.[8,10]

Based on this body of data, we hypothesized that intraperitoneal (IP) administration of CPMV could protect from the onset of metastatic colon tumor growth. We tested this using a mouse model with the IP challenge of CT26 colon cancer cells; CPMV was administered as a soluble injectable in buffer and slow-release hydrogel formulation. In prior work, when used in treatment, we found that prime-boost administrations are needed to achieve potent efficacy and that the need for repeated administrations can be alleviated through formulation as a slow-release injectable.[15] From a clinical point of view, repeated IP administrations are not ideal given the hospitalization requirements for IP injections (IP injections can be given for outpatients after initial surgery to place a port into the abdomen for placement of an IP catheter),[16] which would increase the management cost and worsen the patient's quality of life—already impaired by the consequences of colon cancer disease (such as abdominal pain, change in bowel movements, blood loss and anemia, fatigue, and weight loss).[5] Then, we used CPMV crystals assembled from CPMV and dendrimers;[15] the self-assembled CPMV crystals acted as a depot and extended the CPMV retention time within the IP space, therefore leading to prolonged boosts and potent efficacy after single administration. However, the polyamidoamine (PAMAM) dendrimers are known for dose-limiting toxicity[17,18] that may negatively impact the translational potential of this approach. Thus, there is need to advance the formulation chemistry, and therefore, here, we turned toward the formulation of injectable hydrogels. The purpose of the present study was to use the biocompatible chitosan polymer as a scaffold technology for slow-release formulation of CPMV-based immunotherapeutics.

Chitosan is a family of linear polysaccharides made up of diverse amounts of glucosamine residues produced by deacetylation of the biopolymer chitin.[19] Owing to its excellent biocompatibility and biodegradability, chitosan was initially approved as a generally regarded as safe (GRAS) excipient in 2002 by the European Pharmacopeia 6.0[20] and 10 years later by the 29th edition of the United States Pharmacopeia (USP) 34-NF.[21] Chitosan is currently part of the core excipients in many marketed pharmaceutical formulations such as BST-CarGel intended for cartilage regeneration.[22] Chitosan's cationic character is responsible for most of the attractive pharmaceutical properties of the polymer, including controlled release behavior, mucoadhesion, transfection, permeation enhancement, and *in situ* gelation.[19] Chitosan-based *in situ* gelling formulations are prepared by mixing protonated chitosan with the anionic β-glycerophosphate (GP) salt; the resultant solution appears fluid at or below room temperature but turns into a gel at physiological temperature (37 °C). The thermosensitivity of the chitosan/GP mixture arises from multiple interactions between GP anions and polycationic chitosan chains, including electrostatic binding and increased proton transfer at higher temperature, which leads to reduced chitosan charge density and polymer chain rapprochement, causing gel formation due to hydrophobic inter-chain bonding.[23,24] The *in situ* formed chitosan/GP hydrogels have shown some success as a formulation technology for various biomedical applications, such as local drug delivery for cancers;[23,25] tissue engineering,[26] and controlled release of nanoparticles.[27,28]

In this study, we formulated CPMV nanoparticles in chitosan/GP hydrogels for single-dose IP administration with the goal to prevent colon cancer growth. We assessed the slow-release capability of the hydrogel formulation in the IP space using CPMV labeled with the fluorophore sulfo-cyanine 5 (Cy5)—enabling longitudinal imaging. Finally, we tested the antitumor efficacy of a single-dose CPMV-in-hydrogel formulation (alone or coinjected with soluble CPMV) *versus* single and multiple IP injections of soluble CPMV particles using colon cancer models before disease establishment.

2. EXPERIMENTAL SECTION

2.1. CPMV Production and Modification.

CPMV was propagated in and purified from cowpea plants (*Vigna unguiculata*). For imaging studies, Cy5-labeled CPMV was synthesized, and both CPMV and Cy5-CPMV particles were characterized by ultraviolet–visible (UV–vis) spectroscopy, sodium dodecylsulfate polyacrylamide gel electrophoresis (SDS-PAGE), size exclusion chromatography (SEC), dynamic light scattering (DLS), and transmission electron microscopy (TEM). All protocols were previously described,[29,30] and detailed methods are provided in the Supporting Information (SI) file.

2.2. Hydrogel Preparation and Characterization.

Liquid formulations were prepared by mixing a hydrochloric solution of chitosan with the aqueous solution of sodium GP at room temperature, and CPMV or Cy5-CPMV particles were dispersed in the resultant fluid by vortex mixing. Key formulation properties, such as gelation time, gel swelling, degradation, and release profiles, were determined as previously reported.31 The particulate characteristics of *in vitro* released CPMV particles were

investigated by SEC, DLS, and TEM to confirm particles' integrity. Detailed procedures of hydrogel preparation and characterization are described in the Supporting Information file.

2.3. Animal Studies.

2.3.1. Ethical Statements.—All animal procedures were performed following the guidelines of the Institutional Animal Care and Use Committee (IACUC) of the University of California San Diego (UCSD), using the protocols approved by the UCSD's Animal Ethics committee. We used 7–8 weeks old BALB/c female mice from the Jackson Laboratory (Bar Harbor, ME) and housed the animals at the UCSD Moores Cancer Center with full access to food and water.

2.3.2. In Vivo Release of Cy5-CPMV from Hydrogels.—We injected IP 100 μL of F1–F3 liquid formulations containing 450 μg of Cy5-CPMV or soluble 450 μg of Cy5-CPMV in 100 μL of phosphate-buffered saline (PBS) into shaved healthy mice on day 0 (5 mice per group). We maintained the animals on an alfalfa-free diet starting one week prior to treatment. At predefined time intervals, the IP space was imaged using a Xenogen IVIS 200 optical imaging system (Caliper Life Sciences, Hopkinton, MA), and IVIS software was used for quantitative analysis of fluorescence using the region of interest (ROI). On day 21, mice were sacrificed; major organs (kidneys, liver, lungs, spleen, and heart) were collected for Cy5 fluorescence measurement as mentioned above, and fluorescence intensity was assessed using the ROI.

2.3.3. Body Weight Measurements.—Healthy female BALB/c mice were randomly assigned to one of the following IP treatments ($n = 5$ per group): (i) 200 μg of CPMV, single dose; (ii) 100 μg of CPMV twice (day 0 and 7); (iii) single dose of hydrogel F3 (containing 200 μg of CPMV); (iv) single dose of hydrogel F3 (containing 200 μg of CPMV), followed by 100 μg of CPMV (i.e., F3 + CPMV 100); and then (v) 150 μL of PBS (control group). Body weights were measured every 3–4 days over 28 days as a measure of safety of the formulations.

2.3.4. Colon Cancer Prevention.—CT26-luciferase cells (CT26-Luc cells) were cultured in ATCC-formulated RPMI-1640 medium supplemented with 10% (v/v) fetal bovine serum + antibiotics (Pen–Strep) and maintained at 37 °C in a 5% CO_2 incubator. CT26-Luc cells (1×10^6 in 150 μL of PBS/mouse) were IP-injected into female BALB/c mice. Five IP treatments were tested ($n = 5$ mice per group): immediately after tumor inoculation, (i) soluble CPMV at 200 μg (150 μL of PBS, single dose) and (ii) 100 μg (150 μL of PBS, two weekly injections); for hydrogel formulations, (iii) F3 containing CPMV at 200 μg/150 μL, or (iv) hydrogel without CPMV (blank F3) was injected 30 min before cell inoculation to allow gel formation and avoid cell entrapment in the hydrogel matrix. To prevent any lag-phase effects, an additional group (v) was treated with F3 followed by soluble CPMV at 100 μg/150 μL of PBS. Tumor growth was monitored every 2/3 days using bioluminescence IVIS imaging (5 min post-injection of luciferin at 15 mg mL^{-1}/150 μL of PBS, with a 3 min exposure time) and abdominal circumference measurements. Bioluminescence intensity was calculated using the ROI analysis.

2.4. Statistical Analysis.

All data were processed and analyzed using GraphPad Prism v9.0.2 (GraphPad Software). Comparative analysis was performed by one-way analysis of variance (ANOVA) followed by Tukey's multiple comparison test. Asterisks in the figures indicate statistical differences between a study group and the control (*$p < 0.05$; **$p < 0.01$; ***$p < 0.001$; ****$p < 0.0001$), while hashtags mark statistical differences between study groups ($^{\#}p < 0.05$; $^{\#\#}p < 0.01$; $^{\#\#\#}p < 0.001$).

3. RESULTS AND DISCUSSION

3.1. CPMV/Cy5-CPMV Nanoparticle Production.

CPMV is a plant virus member of the genus *Comovirus* in the family *Comoviridae*. It consists of 60 copies each of small (24 kDa) and large (41 kDa) coat protein (CP) units that self-assemble into an icosahedral particle encapsulating the viral genome composed of two molecules of positive-strand RNA (RNA-1 and RNA-2).[32] The proteinaceous nature of CPMV particles allows multivalent modifications through surface-exposed amino acid handles to impart useful functionalities such as bioimaging capabilities.[33] Using previously published preparation protocols, we produced CPMV particles 55 mg from 100 g of infected leaves of *V. unguiculata* and found the 260/280 nm absorbance ratio of 1.75, which is indicative of good particle purity.[29] To produce fluorescent nanoparticles for *in vivo* release studies, CPMV particles were labeled with the fluorophore Cy5 using the *N*-hydroxysuccinimide (NHS)-activated method to target solvent-exposed lysine side chains, and the conjugate was characterized (Figure S1). The UV–vis spectrum of purified Cy5-CPMV particles exhibited the spectral bands characteristic of the UV–vis absorption features of both the viral capsid protein at 260 nm and the Cy5 dye at 647 nm; we determined that ~30 dyes per CPMV were displayed, previously reported to be ideal for fluorescence bioimaging.[33] Covalent CPMV modification with Cy5 was confirmed by SDS-PAGE, showing that both the small and large CPs were labeled with the dye. Lastly, particle integrity was also confirmed by SEC, which showed a single peak, indicating that Cy5-CPMV's viral components (i.e., CP detected at 260 nm and RNA detected at 280 nm) coeluted with the Cy5 dye (detected at 647 nm) at the same solvent elution volume (11.5 mL) characteristic for CPMV. SEC thus futher confirms covalent conjugation of Cy5 and indicates that intact and pure CPMV-Cy5 was produced; no other prominent peaks for aggregates, free proteins, or unconjugated dyes were apparent. The synthesized Cy5-CPMV particles were used for *in vivo* evaluation of hydrogel release in the peritoneum.

3.2. CPMV-Hydrogel Properties.

The thermosensitivity is the unique property that enables injectable hydrogels to meet key requirements for effective locoregional delivery of therapies:[34] (i) be in a fluid state at room temperature to allow drug incorporation and injection through a small-sized needle (≥23 G), with low viscosity (<1 Pa·s) and (ii) be able to undergo sol-to-gel transition at physiological temperature (37 °C) to enable strong depot formation, avoiding dilution in body fluids, and achieve slow but sustained drug release for prolonged efficacy.

To prepare CPMV-in-chitosan/GP formulations, GP solution (50%) was added to an hydrochloric solution containing either low-, medium-, or high-molecular weight chitosan (2.2%); the addition of GP neutralizes the acidic chitosan solution, resulting in a final pH close to neutral (pH 6.9). After homogenization, the resultant liquid product was vortex-mixed with CPMV solution at room temperature but formed a gel after incubation at 37 °C (Figure 1). Irrespective of whether CPMV or Cy5-CPMV was mixed with the chitosan/GP solution, the formulations composed of high-molecular weight (MW, 1500 kDa) chitosan exhibited the shortest gelation times (5–8 min), while the gelation times for medium-MW (1250 kDa) chitosan formulations were intermediate (8–15 min) and the gelation times of low-MW (250 kDa) chitosan-based formulations were the longest (11–18 min). Formulations composed of low-, medium-, and high-MW chitosan were subsequently named F1, F2, and F3, respectively. The injectability of these formulations was realized by passage through 28, 27, and 26 G needles for F1, F2, and F3, respectively. This ranking is consistent with the viscosity of these liquid formulations we previously recorded at 25 °C (0.099 Pa·s for F1; 0.202 Pa·s for F2; and 0.482 Pa·s for F3).[31] The formulation F3 was found to be the most viscous, but the recorded viscosity value (<1 Pa·s) and passage through a 26 G needle suggest that the F3 formulation has huge potential for good flow and spreading within the TME;[34] other authors established the injectability of a chitosan/GP-based formulation by passing through a 23 G needle.[35]

We used Cy5-CPMV particles to characterize hydrogel degradation, swelling, and release profiles; these data are reported in Nkanga et al.[31] Although no obvious gel degradation or swelling was observed, the UV spectrometric analysis of the release medium revealed continuous release of CPMV particles from the formulated hydrogels. This is consistent with previous observations from scanning electron microscopy of freeze-dried CPMV hydrogels pre- and post-CPMV release.[31] The release rate of CPMV from all the hydrogels was much slower (only 20% released by day 28) compared to that of the controls where CPMV was sampled from PBS (up to 95% was depleted by day 10 due to constant sampling and medium renewal). The fast diffusion of CPMV particles in solution is essentially governed by the Brownian motion, whereas the slow release of CPMV from the hydrogels may reflect the existence of physical or/and chemical hindrances within the polymeric matrix;[36,37] thus, we characterized CPMV particles from hydrogels to verify whether their properties remained unchanged (Figure S2).

The particles size analysis by DLS indicated that the release media from all the hydrogels contained particles with size distribution patterns characteristic of intact CPMV (Figure S2A). SEC was in agreement showing the typical elution profile for CPMV; there was no difference whether freshly prepared *versus* CPMV after a 14-day incubation period, soluble or hydrogel-released, was analyzed—the viral components (RNA and protein) coeluted. Figure S2B compares the chromatographic profiles of CPMV CP detected at 280 nm and indicates that the 260:280 nm absorbance ratios (RNA/protein ratio) remained within the range acceptable for pure and intact CPMV (1.7–1.8).[29] Also, TEM imaging confirmed the presence of intact icosahedral CPMV nanoparticles in the samples withdrawn on day 14 (Figure S3). Collectively, these data verified the stability of CPMV longitudinally released from the hydrogels, which is a commendable asset because the antitumor immunotherapeutic efficacy is contingent on CPMV particulate characteristics.[38,39]

3.3. *In Vivo* Fate of Cy5-CPMV-Hydrogels.

To assess the hydrogel local retention in the IP space, healthy BALB/c mice were IP-injected with a single dose of 450 μg of Cy5-CPMV either dissolved in PBS or dispersed in chitosan/GP liquid formulations made up of low-, medium-, and high-MW chitosan (also denoted as F1, F2, and F3, respectively). Mice were imaged over 21 days post-injection and sacrificed at the endpoint (day 21) for fluorescence analysis of major organs. We observed that soluble Cy5-CPMV particles cleared faster than hydrogel-formulated particles: the free Cy5-CPMV group showed no detectable signal seven (7) days after inoculation, while all the hydrogel (F1–F3) groups exhibited fluorescence until day 21 (Figure 2A). The longitudinal assessment of fluorescence intensity in the IP space revealed a drastic decay for soluble CPMV, while signals from all the hydrogels decreased gradually, indicating a sustained release profile. When compared to both the PBS and soluble CPMV control groups, the fluorescence intensity due to F1 and F3 showed $p < 0.0001$, while the difference with F2 yielded $p < 0.01$, suggesting that the retention time was not contingent on the chitosan molecular weight. Based on its short gelation time and extended-release effect, the hydrogel formulation F3 was selected for antitumor efficacy testing (discussed in the next section). Overall, all the hydrogel formulations demonstrated threefold longer residence time (>21 days) in the peritoneum compared to soluble CPMV, which was cleared within one week. It is worth mentioning that the fluorescence intensity may be underestimated given the dynamic environment and motion within the peritoneum, which may cause premature hydrogel breakage and degradation. In addition, fluorescence quenching may occur; Cy5-CPMV particle entrapment in the hydrogel may have confined fluorescent molecules in proximity, leading to interactions and couplings that cause a partial overlap of light absorption and fluorescence emission and lead to resonant excitation energy transfer processes due to the partial overlap of their curves.[40] Nonetheless, the observed local retention is commendable based on the previously reported data for other slow-release systems, such as the thermosensitive polycaprolactone–poly(ethylene glycol)-based hydrogels[41] and polyamidoamine (PAMAM) dendrimers,[15] which, respectively, achieved 8 and 14 days retention time following IP injections. The fluorescence analysis of organs harvested on day 21 showed no detectable particles in the group injected with soluble particles (Figures 2 and 2B), and this group was not significantly different from the untreated control group. In stark contrast, CPMV-hydrogel groups exhibited high fluorescence signals in the reticulum endothelial system (RES) organs (liver, spleen, kidneys, and lungs), a typical biodistribution profile for CPMV particles.[42,43] This further corroborates the sustained release and prolonged retention of CPMV when formulated as a hydrogel. Importantly, despite the extended retention of the hydrogel in the peritoneum, the IP injection of the high-MW chitosan hydrogel containing 200 μg of CPMV (F3) exhibited negligible influence on healthy mouse body weight variations over 28 days (Figure S5). The data indicated a gradual body weight increase comparable to that observed with soluble CPMV particles and the negative control, which is consistent with biocompatibility of both the proteinaceous CPMV particles[43,44] and chitosan-based hydrogels.[45,46]

3.4. Tumor Prevention Study.

The antitumor prophylactic efficacy of CPMV in the chitosan/GP hydrogel (F3) was assessed in an IP-disseminated colon cancer model (CT26). We inoculated Luc-expressing CT26 cells to BALB/c mice and immediately randomized them into five groups (Figure 3A), which are (i) single-dose blank F3 (hydrogel without CPMV, negative control); (ii) prime and boost dose of 100 μg of CPMV in PBS (day 0 and 7); (iii) single dose of 200 μg of CPMV in PBS; (iv) single dose of 200 μg of CPMV in the hydrogel (F3); and (v) single dose of 200 μg of CPMV in the hydrogel (F3) + 100 μg CPMV in PBS, injected within a 30 min window to allow complete gelation prior to free particle injection, avoiding that the soluble dose would be entrapped in the gel. We monitored tumor growth using bioluminescence imaging and abdominal circumference measurements over 28 days. The model and experimental design were chosen to reflect low tumor burden after surgical debulking; we specifically asked whether CPMV treatment could protect animals from the onset of tumor growth.

The total luminescence in mice treated with F3 + CPMV 100 μg was statistically lower than the total luminescence observed in mice treated with 2× CPMV 100 μg or blank F3 throughout the study period (Figure 3B,C), indicating the excellent tumor growth inhibitory effect of the proposed combination (F3 + CPMV 100 μg) enabling immediate and sustained immune activation through soluble and slowly released CPMV. Mice treated with F3 only also showed reduced luminescence at early timepoints, but disease progression was apparent at later timepoints. Consistent with luminescence measurements, data from abdominal circumference variations indicated that F3 + CPMV 100 μg demonstrated the most potent efficacy against tumor establishment compared to that of any other group (Figure 3D): the abdominal circumference of mice treated with F3 + CPMV 100 μg remained unchanged throughout the study, while there was a gradual increase in the abdominal circumference of mice receiving any other treatment, indicating progressive tumor development due to CT26 cell proliferation (and possible ascites) in the control groups, but not the F3 + CPMV treatment group. This establishes the combination F3 + CPMV 100 μg as a promising antitumor prophylactic treatment for colon cancer. In fact, this approach to supplement slow-release formulations with soluble active ingredients is often adopted to overcome any lag phase; an example includes the depot Risperdal Consta, poly(lactide-*co*-glycolide) (PLGA) microspheres of risperidone.[47]

4. CONCLUSIONS

In this study, we assessed the antitumor preventative efficacy of CPMV in injectable hydrogels made up of chitosan and glycerophosphate. The hydrogel formulation loaded with fluorescent cyanine 5-labeled CPMV exhibited local retention in the intraperitoneal (IP) space, and CPMV released from the hydrogel was detectable over 3 weeks—in stark contrast, soluble CPMV was cleared within one week after administration. Using a colon cancer mouse model, we demonstrate that combined soluble and hydrogel-formulated CPMV is potent to prevent tumor growth after the IP challenge. Codelivery of F3 (CPMV-in-hydrogel) and soluble CPMV 100 μg significantly inhibited the CT26 cell growth over 28 days after tumor cell inoculation and treatment, while soluble single or double dose of

soluble particles failed to prevent tumor growth. The observed antitumor efficacy confirms that CPMV released from hydrogels retained its inherent immunogenicity and highlights the potential of hydrogels and slow-release formulations to improve colon cancer therapy through extended local retention. Potential applications of the CPMV-hydrogels are to prevent the recurrence of disease post-surgery. Plant virus-in-hydrogels are promising for future development of cancer immunotherapies, in particular in the setting of an aggressive disease with a high rate of recurrence such as colon and ovarian cancer.

Supplementary Material

Refer to Web version on PubMed Central for supplementary material.

ACKNOWLEDGMENTS

This work was supported by a grant from NIH R01 CA253615 (to N.F.S.). Steinmetz acknowledges support through the Shaughnessy Family Fund for Nano-ImmunoEngineering (nanoIE) at UCSD. The UCSD Specialized Cancer Center Support P30 Grant 2P30CA023100 is acknowledged for providing access to the small imaging facility. Dr. Sourabh Shukla and Young Hun Chung (UC San Diego) are thanked for the technical help with animal experiments.

REFERENCES

(1). Al-Saraireh YM; Alshammari FOFO; Youssef AMM; Al-Sarayreh S; Almuhaisen GH; Alnawaiseh N; Al-Shuneigat JM; Alrawashdeh HM Cytochrome 4z1 Expression Is Associated with Poor Prognosis in Colon Cancer Patients. OncoTargets Ther. 2021, 14, 5249–5260.

(2). Cancer - WHO, World Health Organization 2022. https://www.who.int/News-Room/Fact-Sheets/Detail/Cancer (accessed Jan 29, 2022).

(3). Siegel RL; Miller KD; Fuchs HE; Jemal A Cancer Statistics, 2021. Ca-Cancer J. Clin 2021, 71, 7–33. [PubMed: 33433946]

(4). Torre LA; Bray F; Siegel RL; Ferlay J; Lortet-Tieulent J; Jemal A Global Cancer Statistics, 2012. Ca-Cancer J. Clin 2015, 65, 87–108. [PubMed: 25651787]

(5). Kuipers EJ; Grady WM; Lieberman D; Seufferlein T; Sung JJ; Boelens PG; Van De Velde CJH; Watanabe T Colorectal Cancer. Nat. Rev. Dis. Primers 2015, 1, No. 15065.

(6). Luo D; Yang Y; Shan Z; Liu Q; Cai S; Li Q; Li X Clinicopathological Features of Stage I–III Colorectal Cancer Recurrence Over 5 Years After Radical Surgery Without Receiving Neoadjuvant Therapy: Evidence From a Large Sample Study. Front. Surg 2021, 8, No. 666400.

(7). You B; Chen EX Anti-EGFR Monoclonal Antibodies for Treatment of Colorectal Cancers: Development of Cetuximab and Panitumumab. J. Clin. Pharmacol 2012, 52, 128–155. [PubMed: 21427284]

(8). Mao C; Beiss V; Fields J; Steinmetz NF; Fiering S Cowpea Mosaic Virus Stimulates Antitumor Immunity through Recognition by Multiple MYD88-Dependent Toll-like Receptors. Biomaterials 2022, 275, No. 120914.

(9). Koellhoffer EC; Mao C; Beiss V; Wang L; Fiering SN; Boone CE; Steinmetz NF Inactivated Cowpea Mosaic Virus in Combination with OX40 Agonist Primes Potent Antitumor Immunity in a Bilateral Melanoma Mouse Model. Mol. Pharmaceutics 2022, 19, 592–601.

(10). Lizotte PH; Wen AM; Sheen MR; Fields J; Rojanasopondist P; Steinmetz NF; Fiering S In Situ Vaccination with Cowpea Mosaic Virus Nanoparticles Suppresses Metastatic Cancer. Nat. Nanotechnol 2016, 11, 295–303. [PubMed: 26689376]

(11). Shukla S; Myers JT; Woods SE; Gong X; Czapar AE; Commandeur U; Huang AY; Levine AD; Steinmetz NF Plant Viral Nanoparticles-Based HER2 Vaccine: Immune Response Influenced by Differential Transport, Localization and Cellular Interactions of Particulate Carriers. Biomaterials 2017, 121, 15–27. [PubMed: 28063980]

(12). Shukla S; Wang C; Beiss V; Steinmetz NF Antibody Response against Cowpea Mosaic Viral Nanoparticles Improves in Situ Vaccine Efficacy in Ovarian Cancer. ACS Nano 2020, 14, 2994–3003. [PubMed: 32133838]

(13). Hoopes PJ; Wagner RJ; Duval K; Kang K; Gladstone DJ; Moodie KL; Crary-Burney M; Ariaspulido H; Veliz FA; Steinmetz NF; Fiering SN Treatment of Canine Oral Melanoma with Nanotechnology-Based Immunotherapy and Radiation. Mol. Pharmaceutics 2018, 15, 3717–3722.

(14). Chung YH; Park J; Cai H; Steinmetz NF S100A9-Targeted Cowpea Mosaic Virus as a Prophylactic and Therapeutic Immunotherapy against Metastatic Breast Cancer and Melanoma. Adv. Sci 2021, 8, No. 2101796.

(15). Czapar AE; Tiu BDB; Veliz FA; Pokorski JK; Steinmetz NF Slow-Release Formulation of Cowpea Mosaic Virus for In Situ Vaccine Delivery to Treat Ovarian Cancer. Adv. Sci 2018, 5, No. 1700991.

(16). Wright AA; Cronin A; Milne DE; Bookman MA; Burger RA; Cohn DE; Cristea MC; Griggs JJ; Keating NL; Levenback CF; Mantia-Smaldone G; Matulonis UA; Meyer LA; Niland JC; Weeks JC; O'Malley DM Use and Effectiveness of Intraperitoneal Chemotherapy for Treatment of Ovarian Cancer. J. Clin. Oncol 2015, 33, 2841–2847. [PubMed: 26240233]

(17). Albertazzi L; Gherardini L; Brondi M; Sulis Sato S; Bifone A; Pizzorusso T; Ratto GM; Bardi G In Vivo Distribution and Toxicity of PAMAM Dendrimers in the Central Nervous System Depend on Their Surface Chemistry. Mol. Pharmaceutics 2013, 10, 249–260.

(18). Mukherjee SP; Lyng FM; Garcia A; Davoren M; Byrne HJ Mechanistic Studies of in Vitro Cytotoxicity of Poly-(Amidoamine) Dendrimers in Mammalian Cells. Toxicol. Appl. Pharmacol 2010, 248, 259–268. [PubMed: 20736030]

(19). Aranaz I; Alcántara AR; Civera MC; Arias C; Elorza B; Caballero AH; Acosta N Chitosan: An Overview of Its Properties and Applications. Polymers 2021, 13, No. 3256.

(20). European Pharmacopoeia Commission and European Directorate for the Quality of Medicines and Healthcare. European Pharmacopoeia, 10th ed.; Council of Europe: Strasbourg, France, 2019.

(21). The United States Pharmacopeial Convention. The United States Pharmacopeia: The National Formulary; The United States Pharmacopeial Convention: Rockville, MD, USA, 2018.

(22). Nephew Smith, CarGel BioScaffold. 2021, https://www.Smith-Nephew.Com/Key-Products/Sports-Medicine/Bst-Cargel/(accessed Dec 3, 2021).

(23). Zhou HY; Jiang LJ; Cao PP; Li JB; Chen XG Glycerophosphate-Based Chitosan Thermosensitive Hydrogels and Their Biomedical Applications. Carbohydr. Polym 2015, 117, 524–536. [PubMed: 25498667]

(24). Cho J; Heuzey MC; Bégin A; Carreau PJ Physical Gelation of Chitosan in the Presence of β-Glycerophosphate: The Effect of Temperature. Biomacromolecules 2005, 6, 3267–3275. [PubMed: 16283755]

(25). Mei E; Chen C; Li C; Ding X; Chen J; Xi Q; Zhou S; Liu J; Li Z Injectable and Biodegradable Chitosan Hydrogel-Based Drug Depot Contributes to Synergistic Treatment of Tumors. Biomacromolecules 2021, 22, 5339–5348. [PubMed: 34813280]

(26). Song K; Li L; Yan X; Zhang W; Zhang Y; Wang Y; Liu T Characterization of Human Adipose Tissue-Derived Stem Cells in Vitro Culture and in Vivo Differentiation in a Temperature-Sensitive Chitosan/β-Glycerophosphate/Collagen Hybrid Hydrogel. Mater. Sci. Eng. C 2017, 70, 231–240.

(27). Peng Q; Sun X; Gong T; Wu CY; Zhang T; Tan J; Zhang ZR Injectable and Biodegradable Thermosensitive Hydrogels Loaded with PHBHHx Nanoparticles for the Sustained and Controlled Release of Insulin. Acta Biomater. 2013, 9, 5063–5069. [PubMed: 23036950]

(28). Li XY; Zheng XL; Wei XW; Guo G; Gou M; Gong CY; Wang XH; Dai M; Chen LJ; Wei YQ; Qian ZY A Novel Composite Drug Delivery System: Honokiol Nanoparticles in Thermosensitive Hydrogel Based on Chitosan. J. Nanosci. Nanotechnol 2009, 9, 4586–4592. [PubMed: 19928122]

(29). Wen AM; Lee KL; Yildiz I; Bruckman MA; Shukla S; Steinmetz NF Viral Nanoparticles for in Vivo Tumor Imaging. J. Visualized Exp 2012, No. e4352.

(30). Wen AM; Shukla S; Saxena P; Aljabali AAA; Yildiz I; Dey S; Mealy JE; Yang AC; Evans DJ; Lomonossoff GP; Steinmetz NF Interior Engineering of a Viral Nanoparticle and Its Tumor Homing Properties. Biomacromolecules 2012, 13, 3990–4001. [PubMed: 23121655]

(31). Nkanga CI; Ortega-Rivera OA; Shin MD; Moreno-Gonzalez MA; Steinmetz NF Injectable Slow-Release Hydrogel Formulation of a Plant Virus-Based COVID-19 Vaccine Candidate. Biomacromolecules 2022, 23, 1812–1825. [PubMed: 35344365]

(32). Saunders K; Sainsbury F; Lomonossoff GP Efficient Generation of Cowpea Mosaic Virus Empty Virus-like Particles by the Proteolytic Processing of Precursors in Insect Cells and Plants. Virology 2009, 393, 329–337. [PubMed: 19733890]

(33). Wen AM; Infusino M; De Luca A; Kernan DL; Czapar AE; Strangi G; Steinmetz N Interface of Physics and Biology: Engineering Virus-Based Nanoparticles for Biophotonics. Bioconjugate Chem. 2015, 26, 51–62.

(34). Al Sabbagh C; Seguin J; Agapova E; Kramerich D; Boudy V; Mignet N Thermosensitive Hydrogels for Local Delivery of 5-Fluorouracil as Neoadjuvant or Adjuvant Therapy in Colorectal Cancer. Eur. J. Pharm. Biopharm 2020, 157, 154–164. [PubMed: 33222768]

(35). Stanzione A; Polini A; La Pesa V; Quattrini A; Romano A; Gigli G; Moroni L; Gervaso F Thermosensitive Chitosan-Based Hydrogels Supporting Motor Neuron-like NSC-34 Cell Differentiation. Biomater. Sci 2021, 9, 7492–7503. [PubMed: 34642708]

(36). Ukmar T; Gaberek M; Merzel F; Godec A Modus Operandi of Controlled Release from Mesoporous Matrices: A Theoretical Perspective. Phys. Chem. Chem. Phys 2011, 13, 15311–15317. [PubMed: 21792392]

(37). Ukmar T; Maver U; Planinšek O; Kaučič V; Gaberšček M; Godec A Understanding Controlled Drug Release from Mesoporous Silicates: Theory and Experiment. J. Controlled Release 2011, 155, 409–417.

(38). Marbrook J; Matthews REF The Differential Immunogenicity of Plant Viral Protein and Nucleoproteins. Virology 1966, 28, 219–228. [PubMed: 4956602]

(39). Murray AA; Wang C; Fiering S; Steinmetz NF In Situ Vaccination with Cowpea vs Tobacco Mosaic Virus against Melanoma. Mol. Pharmaceutics 2018, 15, 3700–3716.

(40). Wen AM; Infusino M; De Luca A; Kernan DL; Czapar AE; Strangi G; Steinmetz NF Interface of Physics and Biology: Engineering Virus-Based Nanoparticles for Biophotonics. Bioconjugate Chem. 2015, 26, 51–62.

(41). Xu S; Fan H; Yin L; Zhang J; Dong A; Deng L; Tang H Thermosensitive Hydrogel System Assembled by PTX-Loaded Copolymer Nanoparticles for Sustained Intraperitoneal Chemotherapy of Peritoneal Carcinomatosis. Eur. J. Pharm. Biopharm 2016, 104, 251–259. [PubMed: 27185379]

(42). Shukla S; Ablack AL; Wen AM; Lee KL; Lewis JD; Steinmetz NF Increased Tumor Homing and Tissue Penetration of the Filamentous Plant Viral Nanoparticle Potato Virus X. Mol. Pharmaceutics 2013, 10, 33–42.

(43). Singh P; Prasuhn D; Yeh RM; Destito G; Rae CS; Osborn K; Finn MG; Manchester M Bio-Distribution, Toxicity and Pathology of Cowpea Mosaic Virus Nanoparticles in Vivo. J. Controlled Release 2007, 120, 41–50.

(44). Lam P; Lin RD; Steinmetz NF Delivery of Mitoxantrone Using a Plant Virus-Based Nanoparticle for the Treatment of Glioblastomas. J. Mater. Chem. B 2018, 6, 5888–5895. [PubMed: 30923616]

(45). Tyliszczak B; Drabczyk A; Kudłacik-Kramarczyk S; Rudnicka K; Gatkowska J; Sobczak-Kupiec A; Jampilek J In Vitro Biosafety of Pro-Ecological Chitosan-Based Hydrogels Modified with Natural Substances. J. Biomed. Mater. Res., Part A 2019, 107, 2501–2511.

(46). Su F; Wang Y; Liu X; Shen X; Zhang X; Xing Q; Wang L; Chen Y Biocompatibility and in Vivo Degradation of Chitosan Based Hydrogels as Potential Drug Carrier. J. Biomater. Sci., Polym. Ed 2018, 29, 1515–1528. [PubMed: 29745306]

(47). Su Z-X; Shi Y; Teng L; Li X; Wang L; Meng Q; Teng L; Li Y-X Biodegradable Poly (D, L-Lactide-Co-Glycolide) (PLGA) Microspheres for Sustained Release of Risperidone: Zero-Order Release Formulation. Pharm. Dev. Technol 2011, 16, 377–384. [PubMed: 20370594]

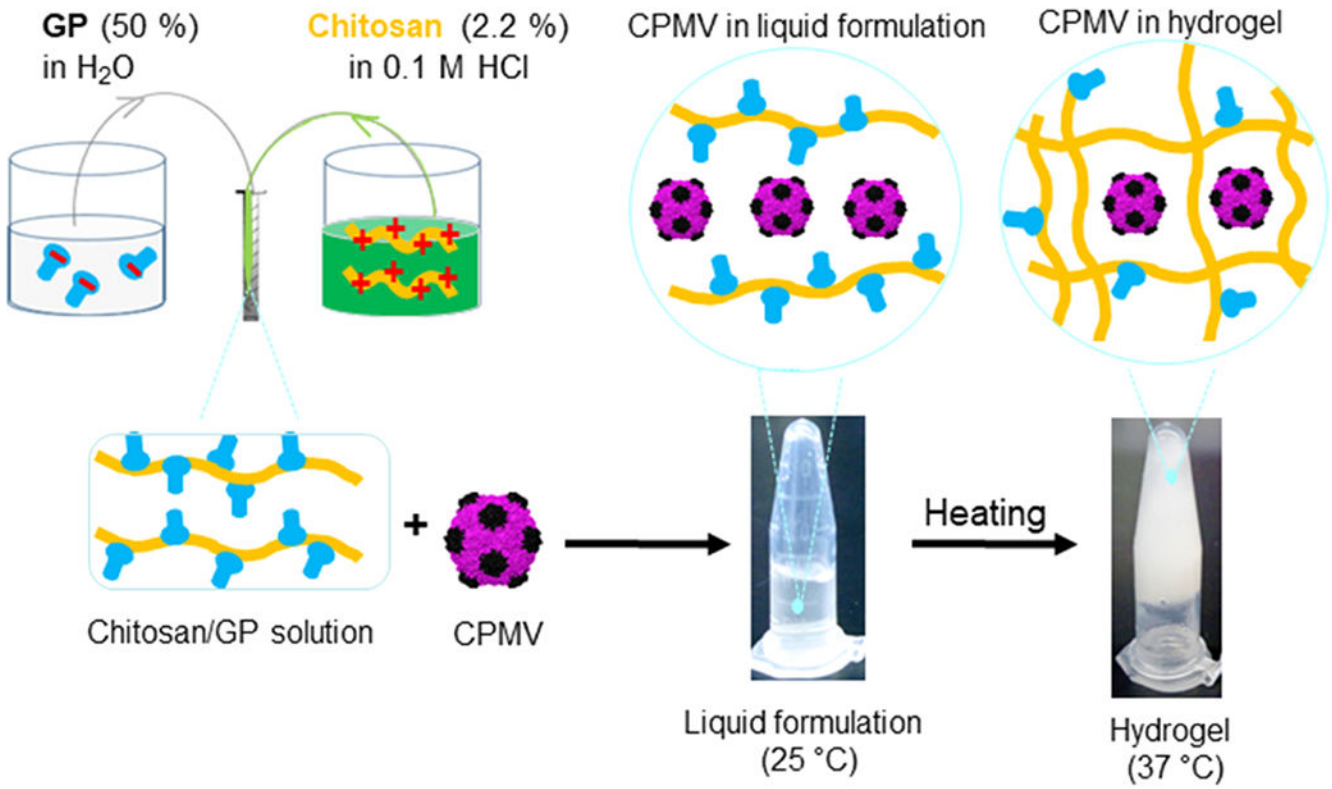

Figure 1.
Schematic presentation of the CPMV formulation in chitosan/GP hydrogels. Images of inverted Eppendorf tubes illustrate the no-flow behavior and increased turbidity occurring when gel forms upon heating.

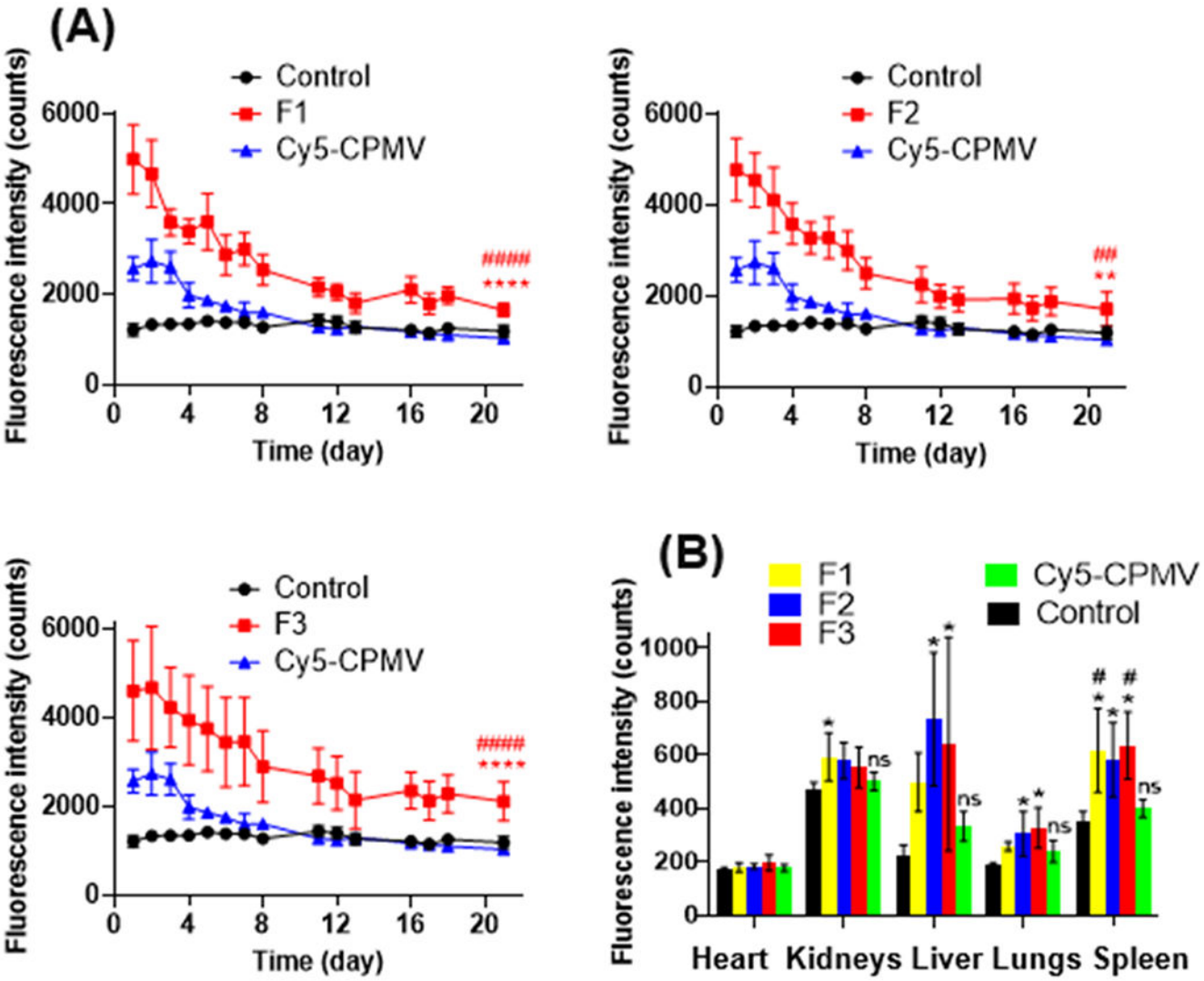

Figure 2.

(A) Fluorescence intensity longitudinally determined using ROI analysis ($n = 5$), tracking the persistence of fluorescence signals from CPMV-Cy5 over 21 days following IP single injection of 450 μg of Cy5-CPMV in PBS (Cy5-CPMV group) or 450 μg of Cy5-CPMV formulated in hydrogels (F1, F2, and F3); the control group was untreated mice. (B) Fluorescence intensity measured by ROI analysis of organs ($n = 5$) collected at the study endpoint (day 21). Asterisks indicate statistical differences *versus* the control (*$p < 0.05$; **$p < 0.01$; ****$p < 0.0001$); hashtags show significant differences between a given hydrogel formulation and soluble Cy5-CPMV ($^{\#}p < 0.05$; $^{\#\#}p < 0.01$; $^{\#\#\#\#}p < 0.0001$), ns denotes not statistically significant.

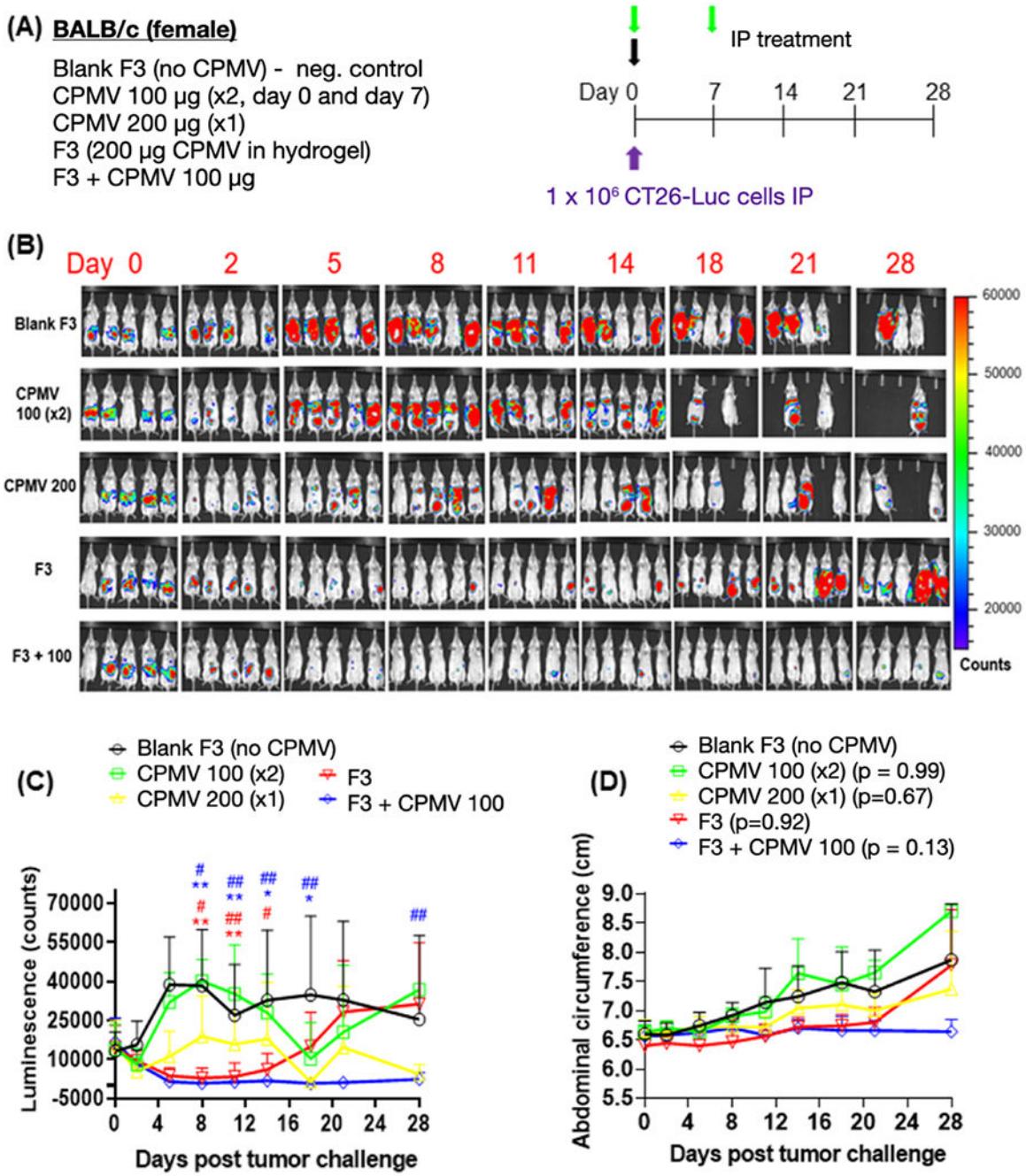

Figure 3.

CPMV-in-chitosan/GP hydrogel inhibits colon cancer growth in the intraperitoneal (IP) space (n = 5 mice per group). (A) Study design: BALB/c mice were inoculated IP with 1 million luciferase-labeled CT26 cells and then treated with single administration of the hydrogel F3 (containing 200 μg of CPMV) only or hydrogel F3 + 100 μg of soluble CPMV in PBS or single administration of 200 μg of soluble CPMV in PBS or prime and boost administration (weekly apart) of 100 μg of soluble CPMV in PBS as a prime-boost regimen. Cancer cell growth was longitudinally assessed by bioluminescence imaging (B)

and intensity measurements (C) in the intraperitoneal space 5 min following I.P. injection of luciferin 15 mg mL^{-1}/150 μL. The luminescence was calculated using ROI analysis from Living Image 3.0 software. Asterisks indicate statistical differences *versus* the control (*$p < 0.05$; **$p < 0.01$); hashtags show significant differences between a given hydrogel treatment and soluble prime-boost CPMV particle ($^{\#}p < 0.05$; $^{\#\#}p < 0.01$). No asterisk/hashtag means that the difference is not statistically significant. Tumor burden and ascites development were monitored by measuring abdominal circumferences (D). The *p* values indicate the difference with the control group (blank F3) on day 28.